Configuration interaction studies on the spectroscopic properties of PbO including spin–orbit coupling*

Wang Luo(罗旺)[1,2], Rui Li(李瑞)[1,†], Zhiqiang Gai(盖志强)[3], RuiBo Ai(艾瑞波)[1], Hongmin Zhang(张宏民)[1], Xiaomei Zhang(张晓美)[2,4], and Bing Yan(闫冰)[2,4,‡]

[1] *College of Science, Qiqihar University, Qiqihar* 161006, *China*
[2] *Institute of Atomic and Molecular Physics, Jilin University, Changchun* 130012, *China*
[3] *Department of Electronic Information, Jiangsu University of Science and Technology, Zhenjiang* 212003, *China*
[4] *Jilin Provincial Key Laboratory of Applied Atomic and Molecular Spectroscopy, Jilin University, Changchun* 130012, *China*

(Received 25 January 2016; revised manuscript received 15 March 2016; published online 27 May 2016)

Lead oxide (PbO), which plays the key roles in a range of research fields, has received a great deal of attention. Owing to the large density of electronic states and heavy atom Pb including in PbO, the excited states of the molecule have not been well studied. In this work, high level multireference configuration interaction calculations on the low-lying states of PbO have been carried out by utilizing the relativistic effective core potential. The effects of the core-valence correlation correction, the Davidson modification, and the spin–orbital coupling on the electronic structure of the PbO molecule are estimated. The potential energy curves of 18 Λ-S states correlated to the lowest dissociation limit (Pb (^3P_g) + O(^3P_g)) are reported. The calculated spectroscopic parameters of the electronic states below 30000 cm^{-1}, for instance, $X^1\Sigma^+$, $1^3\Sigma^+$, and $1^3\Sigma^-$, and their spin–orbit coupling interaction, are compared with the experimental results, and good agreements are derived. The dipole moments of the 18 Λ-S states are computed with the configuration interaction method, and the calculated dipole moments of $X^1\Sigma^+$ and $1^3\Sigma^+$ are consistent with the previous experimental results. The transition dipole moments from $1^1\Pi$, $2^1\Pi$, and $2^1\Sigma^+$ to $X^1\Sigma^+$ and other singlet excited states are estimated. The radiative lifetime of several low-lying vibrational levels of $1^1\Pi$, $2^1\Pi$, and $2^1\Sigma^+$ states are evaluated.

Keywords: lead oxide, MRCI+*Q* method, dipole moments, transitional properties

PACS: 31.50.Df, 31.15.aj, 31.15.ag **DOI:** 10.1088/1674-1056/25/7/073101

1. Introduction

Over the last several decades, the lead oxide molecule (PbO) has received considerable attention of experimental and theoretical studies due to the extensive use in making glass.[1,2] The percentage of PbO in glass can affect the refractive index and the viscosity index of the glass, which can also influence the ability of glass absorbing x-rays. On the other hand, the chemiluminescence spectra of PbO are located in the ultraviolet and visible range, which have been observed in the chemical reaction of atomic Pb with O_3 under single-collision conditions.[3,4] Hence, the electronic structures and transitional properties of low-lying states of PbO can help to understand the detailed reaction mechanisms.

The early experimental investigations mainly focused on the spectroscopic properties of the ground state $X^1\Sigma^+$, $1^3\Sigma^+$, $1^3\Sigma^-$, and $1^3\Pi$. Horiai *et al.*[5] observed the vibration–rotation spectrum in the infrared region using a tunable laser spectrometer, and obtained the Dunham coefficients of $X^1\Sigma^+$. The infrared spectrum of $X^1\Sigma^+$ was photographed by Chertihin and Andrews[6] via chemical reactions of laser ablated Pb and O_2, and the spectroscopic constant of $X^1\Sigma^+$ was evaluated. Knöckel *et al.*[7] used molecular-beam laser spectroscopy to observe the $1^3\Sigma^+$–$X^1\Sigma^+$ transition of PbO, and obtained the precise spectroscopic parameters of the $1^3\Sigma^+$ state. Later, Dorko *et al.*[8] photographed the chemiluminescence of PbO by using the reaction between lead vapor and the $^1\Delta$ excited state of O_2. From the observed vibronic spectrum, they estimated the vibronic molecular constants of $X^1\Sigma^+$, $1^3\Sigma^+$, $1^3\Sigma^-$, $1^3\Pi$, and $2^1\Sigma^+$. DeMille *et al.*,[9] Kawall *et al.*,[10] Hunter *et al.*,[11] and Leanhardt *et al.*[12] adopted a series of new approaches to investigate the molecular dipole moments (DM) and hyperfine constants of $X^1\Sigma^+$ and $1^3\Sigma^+$ states.

Along with the experimental works, a larger number of theoretical studies have been carried out to investigate the electronic structures of the low-lying states of PbO. Chertihin *et al.*[6] and Barandiara *et al.*[13] computed the geometry and vibrational frequency of $X^1\Sigma^+$ employing density functional theory (DFT/B3LYP) and quasi-relativistic *ab initio* model potential method, respectively. Subsequently, Iliaš *et al.*[14] studied the electronic structure of $X^1\Sigma^+$ using a high-level coupled-cluster method with single, double, and noniterative triple excitations (CCSD(T)), and obtained the more

*Project supported by the National Natural Science Foundation of China (Grant Nos. 11404180 and 11574114), the Natural Science Foundation of Heilongjiang Province, China (Grant No. A2015010), the University Nursing Program for Young Scholars with Creative Talents in Heilongjiang Province, China (Grant No. UNPYSCT-2015095), and the Natural Science Foundation of Jilin Province, China (Grant No. 20150101003JC).

†Corresponding author. E-mail: lirei01@163.com
‡Corresponding author. E-mail: yanbing@jlu.edu.cn

© 2016 Chinese Physical Society and IOP Publishing Ltd

accurate spectroscopic constant of $X^1\Sigma^+$. Kello *et al.*[15,16] and Petrov[17] calculated the DM of $X^1\Sigma^+$ using a relativistic high-level-correlated method and a semi-empirical approach, respectively. Navati[18] calculated the potential energy curves of $X^1\Sigma^+$ and $1^3\Pi_1$ using the Morse–Korwar–Navati (MKN) oscillator model. Using the configuration interaction method, Balasubramanian and Pitzer[4] systematically calculated the electronic structures of the 11 electronic states of PbO, applying the relativistic effective core potential. In their calculations, the spin–orbit coupling (SOC) interactions of the low-lying states were also taken into account.

Despite the great many experimental and theoretical works that have been performed over the last few decades, information about the low-lying states of PbO is still too limited. The previous experimental studies were mainly focused on the ground state $X^1\Sigma^+$, $1^3\Sigma^+$, $1^3\Sigma^-$, and $1^3\Pi$, while the previous theoretical investigations were concentrated on $X^1\Sigma^+$ except Ref. [4]. Hence, our knowledge of the other excited states of PbO is still lacking. As illuminated in the literature of the isovalent molecules CS,[19] CSe,[20] and GeO,[21] the low-lying electronic states of PbO present a large density, which can lead to strong coupling interactions of these states. The strong coupling interactions cause more complicated electronic configurations of the excited states, making it a challenge to compute the electronic structure of these states.

In this work, we carry out high-level configuration interaction calculations on the low-lying states of PbO. On the basis of the calculated potential energy curves (PECs) of the low-lying states, the spectroscopic parameters of the bound states are fitted. The radiative lifetimes of several low-lying vibrational levels of $1^1\Pi$, $2^1\Pi$, and $2^1\Sigma^+$ are evaluated.

2. Methods and computational details

In the present study, the electronic structure calculations are performed with the Molpro2010[22] program designed by Werner *et al.* The symmetry group of PbO is $C_{\infty v}$; however, due to the limitation of the Molpro package, the calculations are done in the C_{2v} subgroup. The relationships of the irreducible representations of C_{2v} and $C_{\infty v}$ are $\Sigma^+ = A_1$, $\Pi = B_1 + B_2$, $\Delta = A_1 + A_2$, and $\Sigma^- = A_2$. The single-point energies of the low-lying states are calculated to construct the PECs, where the contracted aug-cc-pwCV5Z-PP[23] with relativistic effective core potential (RECP) ECP60MDF and aug-cc-pwCV5Z[24] basis sets are selected for atoms Pb and O, respectively. With the help of the Winger–Witmer principle, the relationship between 18 low-lying Λ-S states and the lowest dissociation limit is given by

$$\begin{aligned} \mathrm{Pb}(^3\mathrm{P_g}) + \mathrm{O}(^3\mathrm{P_g}) \rightarrow\ & (2^1\Sigma^+ + 2^1\Pi + {}^1\Sigma^- + {}^1\Delta) \\ & + (2^3\Sigma^+ + 2^3\Pi + {}^3\Sigma^- + {}^3\Delta) \\ & + (2^5\Sigma^+ + 2^5\Pi + {}^5\Sigma^- + {}^5\Delta). \end{aligned} \quad (1)$$

In order to obtain the accurate structure of PbO, the energy eigenvalues of the electronic states at a set of internuclear distances are computed through the following three steps. First, the single-configuration wavefunction is calculated by the Hartree–Fock method. Second, the multi-configuration wavefunction is obtained by the state-averaged complete active space self-consistent field (CASSCF) method.[25] Finally, by utilizing the CASSCF energies as the reference, the energy eigenvalues of the Λ-S states are computed with the internally contracted multireference configuration interaction approach (MRCI)[26] including Davison size-extensivity correction (+Q).[27] In the CASSCF and MRCI calculations, the active space is selected as $4A_1$, $2B_1$, and $2B_2$, which are correlated to Pb 6s6p and O 2s2p atomic orbitals. The 5 MOs correlating to the 5d atomic orbital of Pb are placed in the closed shell. That is, there are a total of 20 electrons of PbO taking into account in the electronic correlation calculations.

The SOC effect is taken into consideration through the state interaction method utilizing the full Breit–Pauli Hamilton (H_{BP})[28] operator. The spin–orbit part of the H_{BP} operator can be written as

$$\begin{aligned} \hat{H}^{\mathrm{SO}} = \frac{e^2}{2m_{\mathrm{e}}^2c^2} \sum_i \Bigg[& \sum_K \frac{Z_K}{r_{iK}^3} [\boldsymbol{r}_{iK} \times \boldsymbol{p}_i] \cdot \boldsymbol{s}_i \\ & - \sum_{j \neq i} \frac{1}{r_{ij}^3} [\boldsymbol{r}_{ij} \times \boldsymbol{p}_i] \cdot [\boldsymbol{s}_i + 2\boldsymbol{s}_j] \Bigg], \end{aligned} \quad (2)$$

where e is the electron charge, m_{e} is the electronic quality, c is the speed of light, Z_K is the number of nuclear charges of nucleus K, r_{ij} is the distance between electrons i and j, and $\boldsymbol{r}_{iK} = \boldsymbol{r}_i - \boldsymbol{R}_K$ is the position vector of electron i with respect to nucleus K. In the SOC calculations, the spin–orbit eigenstates are obtained by diagonalizing the $\hat{H}^{\mathrm{el}} + \hat{H}^{\mathrm{so}}$ matrix in the basis of the Λ-S wavefunctions. Additionally, the diagonal $\hat{H}^{\mathrm{el}}$ matrix elements are evaluated by the MRCI+Q method, and the off-diagonal $\hat{H}^{\mathrm{so}}$ matrix elements are generated from the MRCI wavefunctions.

Based on the PECs of the bound and quasibound Λ-S and Ω states, the spectroscopic parameters, including equilibrium bond length R_{e}, harmonic vibrational frequencies ω_{e}, anharmonic vibrational frequencies $\omega_{\mathrm{e}}\chi_{\mathrm{e}}$, balanced rotation constant B_{e} are determined by the numerical solution of the one-dimensional nuclear Schrödinger equations utilizing LeRoy's LEVEL[29] program.

3. Results and discussion

3.1. PECs and spectroscopic properties of Λ-S states

The lowest 18 Λ-S electronic states of PbO, which are correlated to the dissociation limit ($\mathrm{Pb}(^3\mathrm{P_g})$ + $\mathrm{O}(^3\mathrm{P_g})$), are calculated with the MRCI+Q method. The PECs of these Λ-S electronic states are plotted in Fig. 1. It can be seen that the typical bound states ($1^3\Sigma^+$, $1^3\Delta$, $1^3\Sigma^-$, $1^1\Sigma^-$, $1^1\Delta$, $1^3\Pi$, and

$1^1\Pi$) are dominantly located in the excitation energy range of 17500–29000 cm^{-1}, which exhibit deep potential wells. In the excitation energy > 36000 cm^{-1}, there are no typical bound states. The $2^1\Sigma^+$ and $2^3\Pi$ states are weakly bound, which have a shallow potential well ~3000 cm^{-1}. The $2^3\Sigma^+$ and $2^1\Pi$ states are also weakly bound at $R = 2.2$ Å, whereas they become repulsive at a large bond length. The quintet states ($1^5\Pi$, $1^5\Sigma^+$, $2^5\Sigma^+$, $1^5\Delta$, $1^5\Sigma^-$, and $1^5\Pi$) are all typical repulsive states. The spectroscopic parameters of these states are determined by numerical solutions of the radical Schrödinger equations of nuclear motion, and the results are tabulated in Table 1. The previously available results in the literature and the electronic configurations of the bound states are also listed in Table 1.

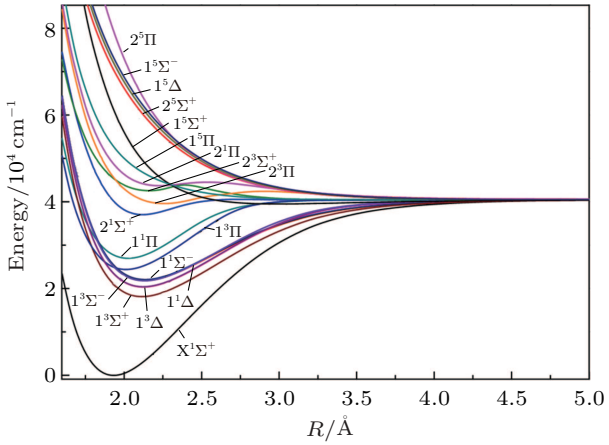


Fig. 1. (color online) The calculated PECs of the low-lying Λ-S electronic states of PbO employing the MRCI+Q method.

Table 1. Computed and experimental spectroscopic parameters of PbO.

State		T_e/cm^{-1}	ω_e/cm^{-1}	$\omega_e x_e$/cm^{-1}	B_e/cm^{-1}	R_e/Å	Electronic configuration at $r = 1.95$ Å
$X^1\Sigma^+$	This work	0	725.1593	2.9293	0.3039	1.9327	$6\sigma^2 7\sigma^2 8\sigma^2 3\pi^4$ (60%)
							$6\sigma^2 7\sigma^2 8\sigma^2 3\pi^3 4\pi^1$ (30%)
	Expt.	0	721.0[a]/720(10)[b]/	3.54[a]	0.3073[a]/	1.9218[a]/	
			720.95736(52)[c]	3.42929(23)[c]	0.30730347(15)[c]		
	Calc.	0	715[d]			2.02[d]	
$1^3\Sigma^+$	This work	18162	540.2700	2.7961	0.2539	2.1146	$6\sigma^2 7\sigma^2 8\sigma^2 3\pi^3 4\pi^1$ (95%)
	Expt.	16132.175[a]/	471.375[a]/	2.4975[b]		2.16[b]	
		16118.5[b]	480(20)[b]				
$1^3\Delta$	This work	20432	530.5106	2.5727	0.2519	2.1230	$6\sigma^2 7\sigma^2 8\sigma^2 3\pi^3 4\pi^1$ (96%)
$1^3\Sigma^-$	This work	21812	519.0418	2.5928	0.2498	2.1321	$6\sigma^2 7\sigma^2 8\sigma^2 3\pi^3 4\pi^1$ (95%)
	Expt.	24665.25[a]	503.5[a]	3.225[a]	0.2495[a]	2.1325[a]	
$1^1\Delta$	This work	21974	515.9020	2.7809	0.2491	2.1348	$6\sigma^2 7\sigma^2 8\sigma^2 3\pi^3 4\pi^1$ (95%)
$1^1\Sigma^-$	This work	22098	513.6828	2.8403	0.2490	2.1354	$6\sigma^2 7\sigma^2 8\sigma^2 3\pi^3 4\pi^1$ (95%)
$1^3\Pi$	This work	24422	585.1766	2.3595	0.2807	2.0113	$6\sigma^2 7\sigma^2 8\sigma^1 3\pi^4 4\pi^1$ (87%)
	Expt.	19862.6[a]/	444.3[a]/420(30)[b]	0.54[a]	0.2586[a]	2.094[a]	
		19894(60)[b]					
$1^1\Pi$	This work	26996	589.2317	2.6505	0.2768	2.0253	$6\sigma^2 7\sigma^2 8\sigma^1 3\pi^4 4\pi^1$ (86%)
							$6\sigma^2 7\sigma^1 8\sigma^2 3\pi^4 4\pi^1$ (5%)
	Expt.	30198.7[a]	530.5[a]	2.92[a]	0.2711[a]	2.046[a]	
	Calc.	27215[d]	521[d]			2.14[d]	

Note: The uncertainty of the experimental figure is given in the bracket. [a]Ref. [31], [b]Ref. [30], [c]Ref. [5], [d]Ref. [4], [e]Ref. [30].

Table 2. Calculated spectroscopic parameters of low-lying Ω states of PbO.

State		T_e/cm^{-1}	ω_e/cm^{-1}	$\omega_e x_e$/cm^{-1}	B_e/cm^{-1}	R_e/Å	Dominant Λ-S states (%) at R_e
$X0^+$	This work	0	721.6657	3.3978	0.3061	1.9260	$X^1\Sigma^+$(98.5)+$1^3\Sigma^-$ (1.5)
	Expt.	0	721.0[a]/720(10)[b]/	3.54[a]/3.42929	0.3073[a]/	1.9218[a]/	
			720.95736(52)[c]	(23)[c]	0.30730347(15)[c]		
	Calc.	0	715[d]			2.02[d]	
$1^3\Sigma_1^+$	This work	15627	507.9586	2.1375	0.2480	2.1395	$1^3\Sigma^+$(71.0)+$1^3\Sigma^-$(29.0)
	Expt.	16024.9[a] /	481.5[a]/480(20)[b]	2.45[a] /2.5[b]	0.252[a]	2.12[a]	
		16051(60)[b]				/2.155(30)[b]	
	Calc.	14551[d]	487[d]			2.23[d]	
$1^3\Sigma_{0-}^+$	This work	16137	505.2296	2.1569	0.2470	2.1441	$1^3\Sigma^+$(74.5)+$^1\Sigma^-$ (25.5)
	Expt.	16454[a]/	441[a] /480(20)[b]	2.49[b]		2.175(30)[b]	
		16321(60)[b]					
	Calc.	14461[d]				2.23[d]	
$1^3\Sigma_{0+}^-$	This work	21697	507.1535	2.0546	0.2466	2.1457	$1^3\Sigma^-$(97.0)+$X^1\Sigma^+$(3.0)
	Expt.	23820[a]	532[a]	3.9[a]	0.254 [a]	2.11[a]	
	Calc.	20747[d]	612[d]			2.23[d]	
$1^3\Sigma_1^-$	This work	23410	500	2.2116	0.2460	2.1482	$1^3\Sigma^-$(71.0)+$1^3\Sigma^+$(29.0)
	Expt.	24947[a]	494[a]	3.0[a]	0.248[a]	2.14[a]	

Note: The uncertainty of the experimental value is tabulated in the bracket. [a]Ref. [31], [b]Ref. [30], [c]Ref. [5], [d]Ref. [4], [e]Ref. [30].

As shown in Table 1, the ground state $X^1\Sigma^+$ is mainly described by the closed-shell configuration $6\sigma^2 7\sigma^2 8\sigma^2 3\pi^4$. Our calculated spectroscopic parameters of $X^1\Sigma^+$ are in good accordance with the latest experimental data. The ω_e, $\omega_e x_e$, and B_e are computed to be 725.1593 cm^{-1}, 2.9293 cm^{-1}, and 0.3039 cm^{-1}, which differ from the corresponding experimental values by only 5.1593 cm^{-1},[30] 0.5000 cm^{-1}, and 0.0034 cm^{-1},[5] respectively; R_e is merely overestimated by 0.0109 Å, as compared to the experimental figure of 1.9218 Å.[5]

The first excited state $1^3\Sigma^+$ originates from the open-shell configuration $6\sigma^2 7\sigma^2 8\sigma^2 3\pi^3 4\pi^1$ corresponding to the $3\pi \rightarrow 4\pi$ one electron excitation. Our calculated T_e is 18162 cm^{-1}, as compared to the previous experimental result of Ω component average of 16118.5 cm^{-1}. The overestimation of 2043.5 cm^{-1} most likely arises from the SOC effect missing in the calculation of the Λ-S state. With comparison to the averaged Ω-component of experimental results,[30,31] the deviations of the calculated ω_e and $\omega_e x_e$ are 60.27 cm^{-1} and 0.2986 cm^{-1}, respectively. The equilibrium distance is calculated to be 2.1146 Å, which is reasonably consistent with the earlier experimental value of 2.16 Å[30] and the theoretical value of 2.23 Å.[4] For the other spectroscopic constants of the Λ-S $1^3\Sigma^+$ state, deviations from the experimental values are shown in Table 1, while better agreement can be expected by introducing the spin-orbit coupling.

The following four excited states $1^3\Delta$, $1^3\Sigma^-$, $1^1\Delta$, and $1^1\Sigma^-$ are mainly described by the electronic configuration $6\sigma^2 7\sigma^2 8\sigma^2 3\pi^3 4\pi^1$. For the four excited states, only the spectroscopic data of $1^3\Sigma^-$ have been reported in the previous investigations. The T_e, ω_e, B_e, and R_e of the $1^3\Sigma^-$ state are calculated to be 21812 cm^{-1}, 519.0418 cm^{-1}, 0.2498 cm^{-1}, and 2.1321 Å, respectively, which are in good agreement with the previous experimental values of the Ω component average of 24665.25 cm^{-1}, 503.5 cm^{-1}, 0.2495 cm^{-1}, and 2.1325 Å.[31] However, the computed $\omega_e x_e$ of $1^3\Sigma^-$ is 2.5928 cm^{-1}, which is 0.6322 cm^{-1} smaller than the experimental value of Ω component average of 3.225 cm^{-1}.[31]

The $1^3\Pi$ and $1^1\Pi$ states both mainly originate from the electronic configuration $6\sigma^2 7\sigma^2 8\sigma^1 3\pi^4 4\pi^1$. The B_e and R_e of $1^3\Pi$ are computed to be 0.2807 cm^{-1} and 2.0113 Å, respectively, being a little larger than the experimental results of 0.2586 cm^{-1} and 2.094 Å. While the calculated T_e = 24422 cm^{-1}, ω_e = 585.1766 cm^{-1}, and $\omega_e x_e$ = 2.3595 cm^{-1} are evidently a departure from the experimental T_e = 19894, ω_e = 420 cm^{-1}, and $\omega_e x_e$ = 0.54 cm^{-1}. The relatively large deviation of $1^3\Pi$ is most probably caused by the SOC between $1^3\Pi$ and other higher Λ-S electronic states. As for the $1^1\Pi$ state, our computed ω_e and B_e are 589.2317 cm^{-1} and 0.2768 cm^{-1}, respectively, which are only 58.7317 cm^{-1} and 0.0057 cm^{-1} larger than the reported experimental values;[31] the values of T_e, $\omega_e x_e$, and R_e are computed to be 26996 cm^{-1}, 2.6505 cm^{-1}, and 2.0253 Å, respectively, which are in reasonable agreement with the previous experimental results of 30198.7 cm^{-1}, 2.92 cm^{-1}, and 2.046 Å.[31]

The permanent dipole moments (DM) of the 18 Λ-S states are also obtained in the MCRI calculations. The variations of DMs with bond lengths are plotted in Fig. 2. At the equilibrium position R_e = 1.9327 of the ground state $X^1\Sigma^+$, the DM of the state is computed to be −1.46 a.u., indicating $Pb^{\delta+}O^{\delta-}$ polarity of the PbO molecule. Compared with the reported experimental value of −1.83 a.u.,[16] our overestimation of 0.37 a.u. may be caused by the deviations in the RECP basis set applied for the Pb atom. At the equilibrium position R_e = 2.1146 of the first excited state $1^3\Sigma^+$, the computed DM of the state is −1.03 a.u., which is in accordance with the latest experimental value of −1.29 a.u.[11] It can be seen from Fig. 2 that the DMs of all 18 Λ-S states tend to zero as internuclear distance $R \rightarrow \infty$, illuminating that the dissociation products are neutral Pb and O atoms.

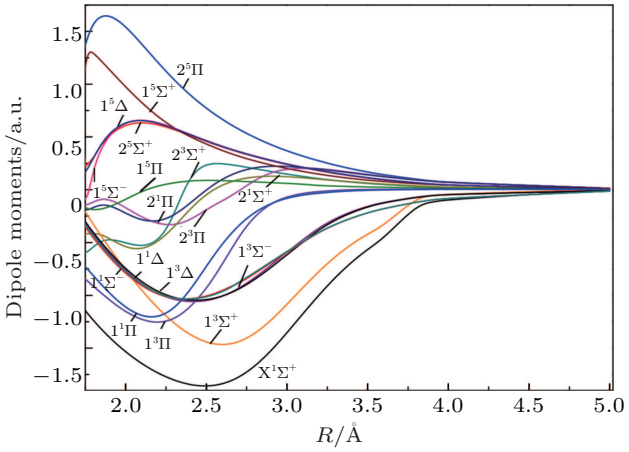


Fig. 2. (color online) Dipole moment curves of low-lying Λ-S states.

3.2. PECs and spectroscopic parameters of Ω states

As is well known, the SOC interactions lead to the energy level splitting of the multiplet state. Especially, for the diatomic molecule containing a heavy atom, the SOC splitting of one multiplet state can reach a size comparable with the energy gap between two different electronic states. In the present study, the SOC is taken into account by perturbation theory using the full Breit–Pauli Hamilton (H_{BP}) operator. In the SOC calculation, the electronic states $X^1\Sigma^+$, $1^3\Sigma^+$, and $1^3\Sigma^-$ are simultaneously included. The three Λ-S states can generate five Ω states ($X^1\Sigma^+_{0+}$, $1^3\Sigma^+_{0-}$, $1^3\Sigma^+_1$, $1^3\Sigma^-_{0+}$, and $1^3\Sigma^-_1$), and the PECs of the five Ω states are plotted in Fig. 3. The calculated spectroscopic parameters of these Ω and the dominant Λ-S state compositions at their equilibrium bond lengths are listed in Table 2.

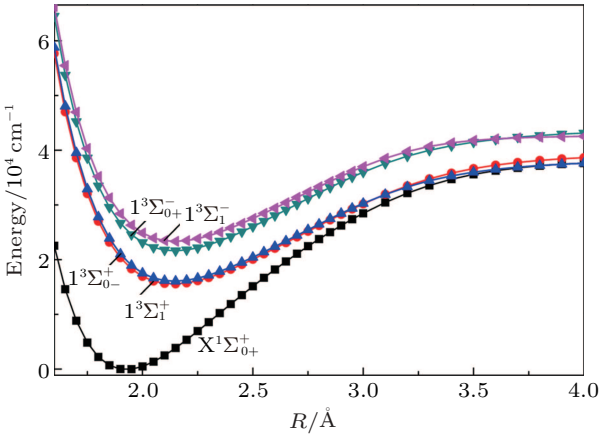


Fig. 3. (color online) The PECs of low-lying Ω states of PbO.

The ground state $X^1\Sigma^+_{0+}$ mainly arises from $X^1\Sigma^+$ (98.5%). Compared with the spectroscopic parameters obtained with the MRCI+Q method, the ω_e, $\omega_e x_e$, B_e, and R_e of the $X^1\Sigma^+_{0+}$ state are corrected by -3.4936 cm^{-1}, 0.4685 cm^{-1}, 0.0022 cm^{-1}, and -0.0067 Å, respectively, which are closer to the reported experimental results of 720 cm^{-1},[30] 3.42929 cm^{-1},[5] 0.30730347 cm^{-1},[5] and 1.9218 Å.[31]

The SOC effect gives rise to the splitting of the triplet state $1^3\Sigma^+$, and two Ω states $1^3\Sigma^+_{0-}$ and $1^3\Sigma^+_1$ are obtained. Both the two Ω states $1^3\Sigma^+_{0-}$ and $1^3\Sigma^+_1$ are generated from Λ-S states $1^3\Sigma^+$ (∼70%) and $1^3\Sigma^-$ (∼30%). The lack of configuration mixing between $1^3\Sigma^+$ and $1^3\Sigma^-$ is probably the main reason of the deviations for the spectroscopic constants of the $1^3\Sigma^+$Λ-S state. The energy separation of $1^3\Sigma^+_{0-}$–$1^3\Sigma^+_1$ is 510 cm^{-1}, which is consistent with the previous experimental measurement of 429.1 cm^{-1}.[31] However, the present calculated energy separation of $1^3\Sigma^+_{0-}$–$1^3\Sigma^+_1$ has a large departure from the experimental value of 270 cm^{-1},[30] which has a large error bar (120 cm^{-1}). For $1^3\Sigma^+_{0-}$ and $1^3\Sigma^+_1$, the calculated T_e are only underestimated by 424 cm^{-1} (2.6%) and 184 cm^{-1} (1.1%), as compared with the experimental T_e of 16051(60) cm^{-1} and 16321(60) cm^{-1}.[30] The calculated R_e of $1^3\Sigma^+_{0-}$ and $1^3\Sigma^+_1$ are only 0.0155 Å (0.7%) and 0.0309 Å (1.4%) shorter than the most recent experimental results of 2.155 Å and 2.175 Å.[30] The ω_e of $1^3\Sigma^+_1$ is calculated to be 507.9586 cm^{-1}, which is larger than the experimental result (480(20) cm^{-1}) by 27.9586 cm^{-1}(5.8%).[30] Moreover, our calculated ω_e (507.9586 cm^{-1}) of $1^3\Sigma^+_1$ is well consistent with the upper limit of error bar of the experiment (500 cm^{-1}).[30] Compared with the experimental results,[30] our calculated deviation of ω_e of $1^3\Sigma^+_1$ (27.9586 cm^{-1} (5.8%)) is slightly larger than that of the previous theoretical result (7 cm^{-1}(1.5%)),[4] but the calculated deviations of T_e and R_e of $1^3\Sigma^+_1$ are only 184 cm^{-1} (1.1%) and 0.0309 Å (1.4%), which are evidently smaller than those of the previous theoretical results of 1860 cm^{-1} (11.4%) and 0.055 Å (2.5%).[4]

Taking into account the SOC effect, the triplet state $1^3\Sigma^-$ splits into two Ω states $1^3\Sigma^-_{0+}$ and $1^3\Sigma^-_1$. The $1^3\Sigma^-_{0+}$ is composed of $1^3\Sigma^-$ (97%) and $X^1\Sigma^+$ (3%), while $1^3\Sigma^-_1$ is generated from $1^3\Sigma^-$ (71%) and $1^3\Sigma^+$ (29%). The energy separation of $1^3\Sigma^-_{0+}$–$1^3\Sigma^-_1$ is 1713 cm^{-1}, as compared with the experimental figure of 1127 cm^{-1}. The overestimation of 586 cm^{-1}is most likely caused by the relatively few electronic states $X^1\Sigma^+$, $1^3\Sigma^+$, and $1^3\Sigma^-$ included in the SOC calculations. For $1^3\Sigma^-_{0+}$, the calculated T_e, ω_e, and R_e are 21697 cm^{-1}, 507.1535 cm^{-1}, and 2.1457 Å, respectively, which are closer to the experimental results of 23820 cm^{-1}, 532 cm^{-1}, and 2.11 Å[31] than the previous theoretical results of 20747 cm^{-1}, 612 cm^{-1}, and 2.23 Å.[4] For $1^3\Sigma^-_1$, the calculated T_e is 1537 cm^{-1} (6.2%) smaller than the experimental value of 24947 cm^{-1};[31] the computed ω_e and R_e are 6 cm^{-1} (1.2%) and 0.0082 Å (0.4%) larger than the experimental results of 494 cm^{-1} and 2.14 Å.[31]

3.3. Transitional properties and radiative lifetimes

The transition dipole moments (TDMs) of some transitions to the ground state $X^1\Sigma^+$ and several low-lying excited states are computed as a function of bond length R. The TDM curves of $1^1\Pi$–$X^1\Sigma^+$, $2^1\Pi$–$X^1\Sigma^+$, $2^1\Sigma^+$–$X^1\Sigma^+$, $2^1\Sigma^+$–$1^1\Pi$, $2^1\Sigma^+$–$2^1\Pi$, and $2^1\Pi$–$1^1\Pi$ transitions are mapped in Fig. 4.

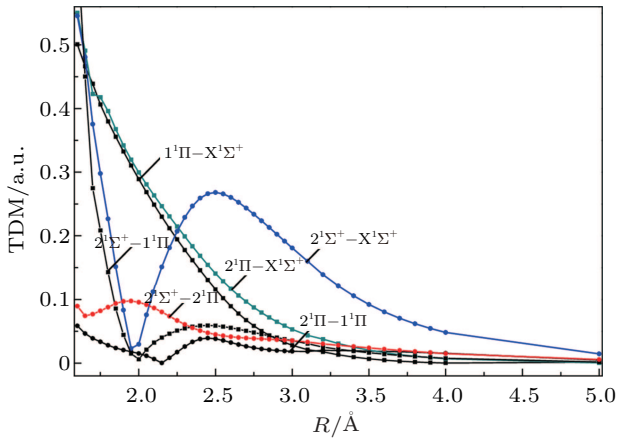


Fig. 4. (color online) The transition dipole moment between singlet states of PbO.

As depicted in Fig. 4, in the Franck–Condon region (1.75 Å–2.25 Å), both TDMs of $1^1\Pi$–$X^1\Sigma^+$ and $2^1\Pi$–$X^1\Sigma^+$ transitions have large values (> 0.23 a.u.), while the TDM of the $2^1\Sigma^+$–$X^1\Sigma^+$ transition decreases rapidly as the Pb–O distance increases and then gradually increases at large internuclear distance. Hence, the TDM curve of the $2^1\Sigma^+$–$X^1\Sigma^+$ transition exhibits a minimum around the equilibrium distance. In general, the calculated TDMs of the $1^1\Pi$–$X^1\Sigma^+$ transition are obviously larger than those of the $2^1\Sigma^+$–$X^1\Sigma^+$ transition in the Franck–Condon region. On the basis of TDMs, the Franck–Condon factors (FCF), and the vibrational energy difference

between higher and lower electronic states, the radiative lifetime of the vibrational level of the excited state is calculated with the following formula:

$$\begin{aligned}\tau &= (A_{v'})^{-1} \\ &= \frac{3h}{64\pi^4 |a_0 e\mathrm{TDM}|^2 \sum_{v''} q_{v'v''} (\Delta E_{v'v''})^3} \\ &= \frac{4.936 \times 10^5}{|\mathrm{TDM}|^2 \sum_{v''} q_{v'v''} (\Delta E_{v'v''})^3}, \end{aligned} \quad (3)$$

where TDM is the averaged electronic transition dipole moment in atomic unit, $q_{v'v''}$ is the FCF between vibrational energy levels v' and v'', and $\Delta E_{v'v''}$ is the energy difference of vibrational energy levels v' and v''. The calculated lifetimes of the five lowest vibrational levels of $1^1\Pi$, $2^1\Pi$, and $2^1\Sigma^+$ states are listed in Table 3. The lifetimes of the low-lying states of PbO have not been reported in the previous experimental and theoretical works. While the lifetimes of isovalent molecule SnO[32] have been computed by Giri *et al.* using multireference singles and doubles configuration interaction (MRDCI) method, and the calculated lifetimes of $A^1\Pi$ and $E^1\Sigma^+$ of SnO were on the order of 10^{-7} s and 10^{-8} s. In this work, the MRCI computed radiative lifetimes of $1^1\Pi$ and $2^1\Sigma^+$ at the low-lying vibrational levels are on the order of 10^{-7} s and 10^{-6} s, respectively. The lifetimes of $1^1\Pi$ of PbO and those of $A^1\Pi$ of SnO[32] are on the same order, however, the lifetimes of $2^1\Sigma^+$ of PbO are two orders of magnitude larger than those of $E^1\Sigma^+$ of SnO.[32] As shown in Eq. (3), the radiative lifetime is directly proportional to the reciprocal of TDM, FCF, and $\Delta E_{v'v''}$. The equilibrium distance of $1^1\Pi$ is close to that of $2^1\Sigma^+$, so the FCFs of the $1^1\Pi$–$X^1\Sigma^+$ and $2^1\Sigma^+$–$X^1\Sigma^+$ transitions are almost the same. As discussed in the properties of TDMs, the TDMs of the $1^1\Pi$–$X^1\Sigma^+$ transition are obviously larger than those of the $2^1\Sigma^+$–$X^1\Sigma^+$ transition, and the $\Delta E_{v'v''}$ of the $1^1\Pi$–$X^1\Sigma^+$ transition is slightly smaller than that of the $2^1\Sigma^+$–$X^1\Sigma^+$ transition, which make the radiative lifetimes of $1^1\Pi$ smaller than those of $2^1\Sigma^+$.

Table 3. Radiative lifetimes of several electronic states at low-lying vibrational levels of PbO.

Transition	Partial lifetime of upper vibrational level					Lifetime of $v'=0$ level of upper state
	$v'=0$	$v'=1$	$v'=2$	$v'=3$	$v'=4$	
$1^1\Pi$–$X^1\Sigma^+$	2.88(–7)	2.92(–7)	2.95(–7)	2.97(–7)	3.00(–7)	$\tau(1^1\Pi) = 2.88(-7)$
$2^1\Sigma^+$–$X^1\Sigma^+$	5.03(–6)	5.14(–6)	5.28(–6)	5.28(–6)	5.71(–6)	$\tau(2^1\Sigma^+) = 5.03(-6)$
$2^1\Pi$–$X^1\Sigma^+$	8.95(–8)	9.62(–8)	1.17(–7)			$\tau(1^1\Pi) = 8.95(-8)$

4. Conclusion

In summary, high-level MRCI+Q calculations on the 18 Λ-S states correlating to the lowest dissociation limitation of PbO have been carried out. The PECs of the low-lying Ω states ($X^1\Sigma^+_{0+}$, $1^3\Sigma^+_{0-}$, $1^3\Sigma^+_{-}$, $1^3\Sigma^-_{0+}$, and $1^3\Sigma^-_{1}$) are computed by employing the state interaction method with the aid of the Breit–Pauli operator. From the PECs of the bound states, the corresponding spectroscopic parameters are evaluated by solving the nuclear Schrödinger equations, and found to be in good accord with the reported experimental results. The permanent DMs of the 18 Λ-S states are determined by the MRCI method. Our calculated permanent DMs of the ground state $X^1\Sigma^+$ and $1^3\Sigma^+$ are −1.46 a.u and −1.03 a.u., respectively, which are consistent with the experimental measurements of −1.83 a.u. and −1.29 a.u. The TDMs of three singlet states ($1^1\Pi$, $2^1\Pi$, and $2^1\Sigma^+$) to the ground state $X^1\Sigma^+$ and other low-lying exited states are investigated. Based on TDMs, FCFs, and energy differences between higher and lower vibrational levels, the radiative lifetimes of the five lowest vibrational levels of $1^1\Pi$, $2^1\Pi$, and $2^1\Sigma^+$ states are determined. The present theoretical investigations reveal more detailed information on the electronic structures and transitional properties of the PbO molecule.

Acknowledgment

We acknowledge the High Performance Computing Center (HPCC) of Jilin University and Qiqihar University for the supercomputer time.

References

[1] Saddeek Y B, Aly K A and Bashier S A 2010 *Physica B* **405** 2407
[2] Hynes M J and Jonson B 1997 *Chem. Soc. Rev.* **26** 133
[3] Oldenborg R C, Dickson C R and Zare R N 1975 *J. Mol. Spectrosc.* **58** 283
[4] Balasubramanian K and Pitzer K S 1983 *J. Phys. Chem.* **87** 4857
[5] Horiai K and Uehara H 1989 *J. Mol. Spectrosc.* **136** 56
[6] Chertihin G V and Andrews L 1996 *J. Chem. Phys.* **105** 2561
[7] Knöckel H and Tiemann E 1984 *Chem. Phys. Lett.* **104** 83
[8] Dorko E A, Glessner J W, Ritchey C M, Rutger L L, Pow J J, Brasure L D, Duray J P and Snyder S R 1986 *Chem. Phys.* **102** 349
[9] DeMille D, Bay F, Bickman S, Kawall D, Krause D, Maxwell S E and Hunter L R 2000 *Phys. Rev. A* **61** 052507
[10] Kawall D, Bay F, Bickman S, Jiang Y and DeMille D 2004 *Phys. Rev. Lett.* **92** 133007
[11] Hunter L, Maxwell S, Ulmer K, Charney N, Peck S, Krause D, Ter-Avetisyan S and DeMille D 2002 *Phys. Rev. A* **65** 030501
[12] Leanhardt A E, Bohn J L, Loh H, Maletinsky P, Meyer E R, Sinclair L C, Stutz R P and Cornell E A 2011 *J. Mol. Spectrosc.* **270** 1
[13] Barandiara Z and Seijo L 1994 *J. Chem. Phys.* **101** 4049
[14] Iliaš M, Aa. Jensen H J, Kellö V, Roos B O and Urban M 2005 *Chem. Phys. Lett.* **408** 210
[15] Kellö V and Sadlej A J 1993 *J. Chem. Phys.* **98** 1345
[16] Kellö V, Sadlej A J and Fægri K 1998 *J. Chem. Phys.* **108** 2056
[17] Petrov A N 2011 *Phys. Rev. A* **83** 024502

[18] Navati B S and Korwar V M 1986 *Physica B+C* **138** 205
[19] Li R, Wei C L, Sun Q X, Sun E P, Xu H F and Yan B 2013 *J. Phys. Chem. A* **117** 2373
[20] Li R, Sun E P, Jin M X, Xu H F and Yan B 2014 *J. Phys. Chem. A* **118** 2629
[21] Liu X J, Miao F J, Li R, Zhang C H, Li Q N and Yan B 2015 *Acta Phys. Sin.* **64** 123101 (in Chinese)
[22] Werner H J, Knowles P J, Knizia G, *et al.* 2010 *MOLPRO: a Package of ab initio Programs*
[23] Peterson K A and Yousaf K E 2010 *J. Chem. Phys.* **133** 174116
[24] Peterson K A and Dunning T H 2002 *J. Chem. Phys.* **117** 10548
[25] Werner H J and Knowles P J 1985 *J. Chem. Phys.* **82** 5053
[26] Werner H J and Knowles P J 1988 *J. Chem. Phys.* **89** 5803
[27] Langhoff S R and Davidson E R 1974 *Int. J. Quantum Chem.* **8** 61
[28] Berning A, Schweizer M, Werner H J, Knowles P J and Palmieri P 2000 *Mol. Phys.* **98** 1823
[29] Le Roy R J 2002 *LEVEL* 7.5: *a Computer Program for Solving the Radial Schröinger Equation for Bound and Quasibound Levels* (University of Waterloo, Chemical Physics Research Report CP-655)
[30] Polak M L, Gilles M K, Gunion R F and Lineberger W C 1993 *Chem. Phys. Lett.* **210** 55
[31] Huber K P and Herzberg G 1979 *Molecular Spectra and Molecular Structure IV, Constants of Diatomic Molecules* (New York: Van Nostrand-Reinhold)
[32] Giri D, Buenker R J and Das K K 2002 *J. Phys. Chem. A* **106** 8790